

Determination of Grouting Defects in "Deep" PT Ducts Using Gamma Rays

Mario A.J. Mariscotti¹, Paul Kelly², Joaquín Boselli¹, Teresita Frigerio¹, Marcelo Ruffolo¹ and Peter Thieberger¹

¹THASA

Reclus 2017, 1609 Boulogne, BA, Argentina
+54-11-4719-5132, mariscotti@thasa.com

²Simpson, Gumpertz & Heger

41 Seyon Street, Building 1, Waltham, MA 02453
781.907.9332 direct, PLKelley@sgh.com

INTRODUCTION

Measurements of grouting condition in PT ducts using gamma rays and gammagraphic plates have been previously reported (1, 2). This method has proved to be adequate for such purpose when the thickness of the concrete specimen, such as a girder, is less than 1.5 ft.

When the ducts are in larger structures, it is necessary to seek a technological alternative. This paper describes an adaptation of THASA's technology to satisfy a request to determine the possible existence of voids and defective grout in ducts in a pier cap 49'-5.5" long and 9'-6" thick. Since it is the center of the cap that sits on the pier, the ducts reach their maximum altitude at the center of the cap and the section of interest is at this high point where the tendon occupies the lower part of the duct.

Six samples that replicate ducts of this kind with different grouting densities, voids and tendons were prepared by Simpson, Gumpertz & Heger (SGH) from Waltham MA..

THE METHODOLOGY

The technique used in this work is called THATIR (3) and its application to the present case is schematically shown in Figure 1. A radioactive source and a small gamma-ray detector-spectrometer are moved down along two 1" diameter vertical holes separated a distance D, on each side of the duct to be inspected. A stepper motor driven by a computer moves the system at regular intervals in space and time and the gamma-ray intensity reaching the detector is recorded and analyzed.

The black area inside the duct (circle in Figure 1) represents the strands, which at the "high point" of the duct are packed down in the lower section of it. The dark and light blue areas represent zones of "hard" and "soft" grout, respectively while the upper section is shown with an air void (white area).

Gamma rays are attenuated and absorbed by matter. The intensity of a gamma ray beam traversing a sample is a function of the thickness times the density of the elements within the sample. Thus an empty zone in the duct will produce an increment of the recorded gamma-ray intensity while gamma rays going through the strands will be more attenuated than if they go through the same thickness of concrete.

The THATIR system includes the following components: a) a frame that supports the displacement axis and a stepper motor, and an arm that holds the tubes containing the source and the detector; b) a power unit; c) a multichannel analyzer and d) a notebook computer.

The detector-spectrometer is connected to a multichannel analyzer that records the gamma-ray spectra of the source in the notebook memory. By measuring the energy of the transmitted gamma rays it is possible to filter out most of the unwanted radiation scattered in the concrete.

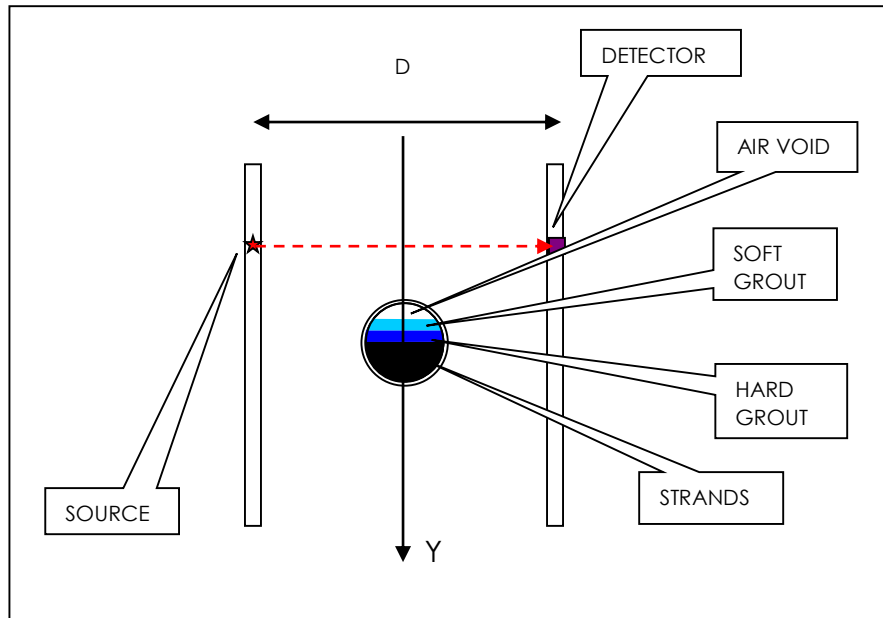


Figure 1: Illustration of the THATIR concept.

EXPERIMENTAL ARRANGEMENT AND MEASUREMENTS

As mentioned, duct samples were prepared by SGH. Figure 2 shows the ducts dimensions and the quantity S used in the main text to indicate the duct section at which measurements were performed.

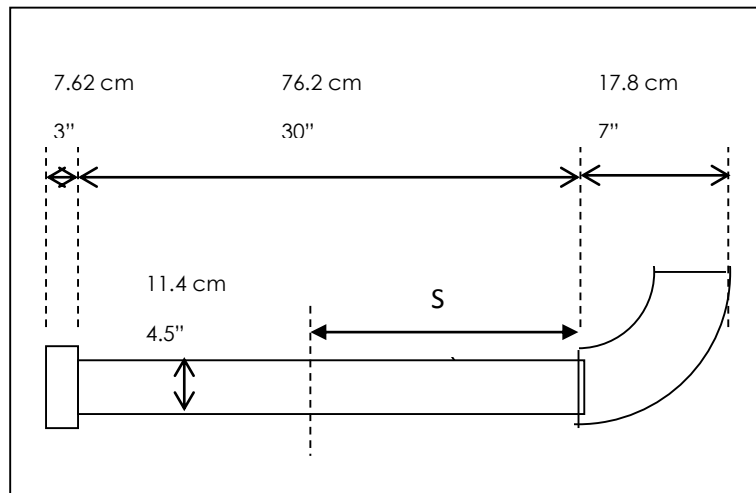


Figure 2: Schematic of ducts used in this work.

Figure 3 shows a picture of the experimental arrangement. The duct samples were placed in the center of a volume of concrete blocks. The purpose of these blocks is to replicate the conditions of a real measurement since gamma rays traversing matter suffer collisions that affect the resolution and sensitivity of the measurements. On top of these blocks sits the mechanism that drives down the tubes containing the source and the detector into the concrete.



Figure 3: Experimental set up. Concrete blocks surround one of the duct samples. On top is THATIR's driving mechanism that moves down the tubes containing the detector (in red) and the source (in white) on each side of the duct.

All measurements were performed with a 123 mCi ^{137}Cs source and a gamma-ray detector-spectrometer with a $\sim 1 \text{ cm}^3$ (0.06 ci) BGO crystal scintillator and a 1024 channel multichannel analyzer. Source-detector distance D was varied but the results discussed in this report correspond to $D = 36.3 \text{ cm}$ (14.3"). Every measurement covered a vertical distance of 20 cm (7.87") at 1mm (0.04") intervals, amounting to 200 data points and a total time of about 4 minutes. Measurements were carried out with the six samples at two different sections $S = 30$ and 45 cm (11.8" and 17.7") where S is as defined in Figure 2.

RESULTS

The results shown in the following correspond to two of the most illustrative examples concerning the sensitivity and resolution of the THATIR method.

The results of interest are the values of the "transition points" (TP) or boundaries between air void-soft grout-hard grout and tendon as indicated in Figure 4 in capital letters (A, B, C...), and the density values in each case.

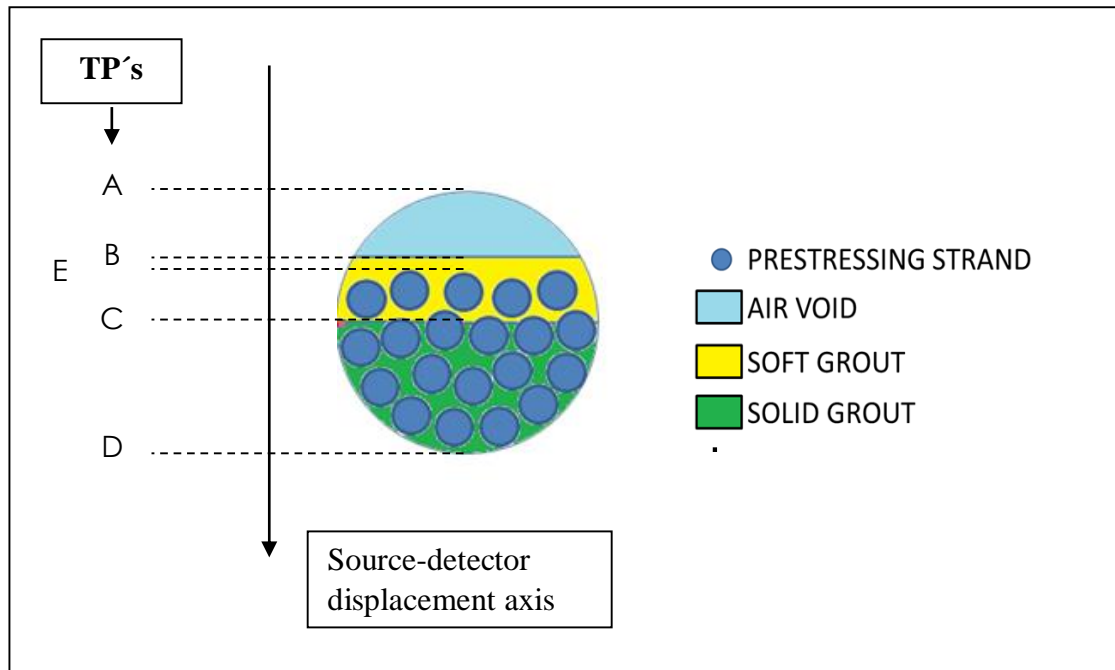


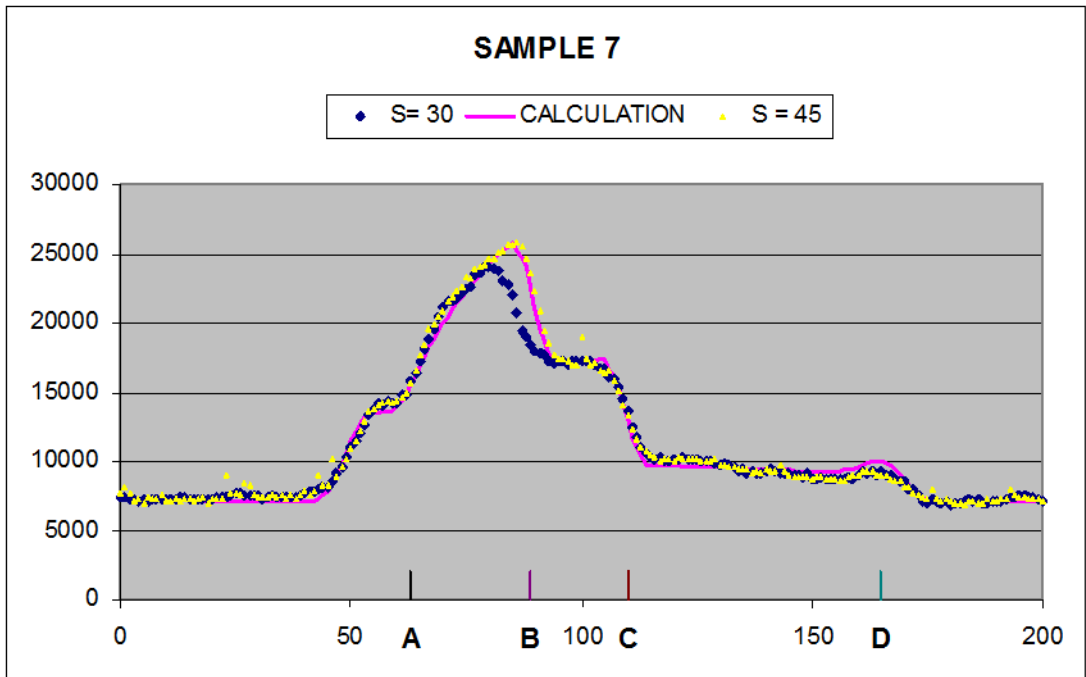
Figure 4: Transition points adjusted in the model calculation to fit the data together with the densities of the soft grout, solid grout and strands.

Figures 5 and 6 show the results obtained for a sample without and with, tendon, respectively.

The plots in the upper part of these figures show data points corresponding to two different sections of the samples at $S = 30$ and 45 cm (see Figure 2) in blue and yellow, respectively. The magenta line represents the result of a calculation in which the positions of transition points and densities were varied to fit the measured data. Those that best fit the data are the outcome of interest and are shown in the tables in the lower part of Figure 5 and 6.

The vertical axis of the plots in Figures 5 and 6 denote the number of counts registered by the detector, while the abscissa corresponds to the downward displacement Y of the source-detector system, in mm. Below the plots are two tables indicating the values of the Transition Points and densities obtained from the fitting process.

The interpretation of the plotted data in Figure 5 is as follows: From $Y = 0$ to approximately $Y = 50$ mm the number of counts is constant; this is the interval where there is only concrete. There is an increase of counts up to point A due to the unavoidable (in the present modular mock up) air gap between the concrete and the top of the duct at A. The subsequent increment in counts is due to the air void zone within the duct. The data for $S = 45$ cm (17.7") (yellow points and magenta line) reaches its maximum at B ($Y = 89$ mm). This marks the boundary with the soft grout. Note that the maximum for $S = 30$ cm (11.8") data occurs at a lower value $Y = 85$ mm indicating that in this section the soft grout band is broader. The number of counts at the plateau around $Y = 100$ determines the density of the soft grout. At point C ($Y = 110$ mm) is the boundary of the hard grout whose density is approximately constant (as it is the number of counts) until point D ($Y = 163$ mm). After that, for $Y > D$ the system enters the zone of concrete below the duct. When comparing the results (the values in tables below plot) with those of the manufacturer's (SGH) the agreement is within 2 mm and 0.1 g/cm^3 in boundaries heights and material densities, respectively. The fact that the data does not exhibit abrupt changes at the TP's is due to the finite size of the detector, but this does not affect the accuracy of the results.



Calculation is for S=45. Label B corresponds to this fit.

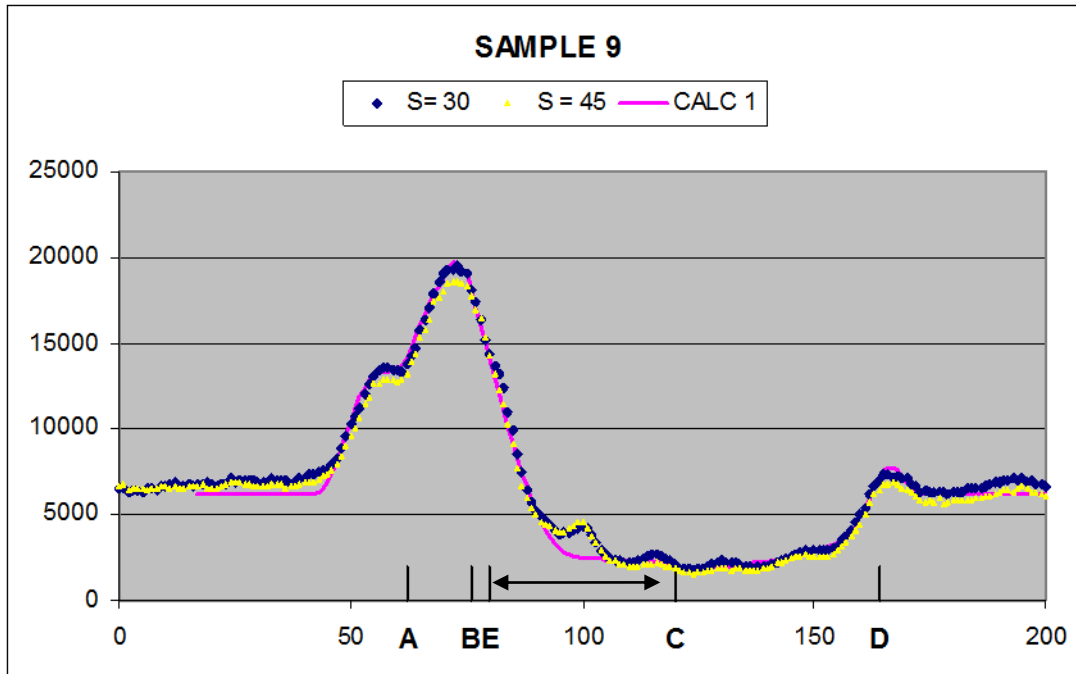
Table a: Identification of TP's (mm / inches)

	Section S (cm)	Top of duct (internal) (A)	Interface air void-soft grout (B)	Interface soft-hard grout (C)	Top strand(s) (E)	Bottom of duct (internal) (D)
Position of TP	30	61	85	110	none	163
	45	61	89	110		163
Distance from bottom	30	102 / 4	78 / 3.1	53 / 2.1		0
	45	102 / 4	74 / 2.9	53 / 2.1		0

Table b: Densities (g/cm²)

Concrete	Duct	Air void	Soft grout	Hard grout	Strands
2.12	1.2	0.4	1.15	1.95	---

Figure 5: Results for sample 7. This sample does not have strands. The measured data at S = 30 cm (blue points) and 45 cm (yellow points) are fitted with a calculation (magenta line) of the number of counts by varying boundaries (TP's) between zones (air void and soft and hard grout) and their densities.



Calculation is for S=30. Uncertainty in C is indicated with the double arrow.

Table a: Identification of TP's (mm / inches)

	Section S (cm)	Top of duct (internal) (A)	Interface air void-soft grout (B)	Interface soft-hard grout (C)	Top strand(s) (E)	Bottom of duct (internal) (D)
Position of TP	30	62	76	83-120	85-80	164
	45	62	76	83-120	85-80	164
Distance from bottom	30	102 / 4.0	88 / 3.5	81-54 / 3.2-2.2	85-80/3.4-3.1	0
	45	102 / 4.0	88 / 3.5	81-54 / 3.2-2.2	85-80/3.4-3.1	0

Table b: Densities (g/cm²)

Concrete	Duct	Air void	Soft grout	Hard grout	Strands
2.2	1.2	0.4	1.2	2.1	5

Figure 6: Results for sample 9. This sample has strands. The measured data at S = 30 cm (blue points) and 45 cm (yellow points) are fitted with a calculation (magenta line) of the number of counts by varying boundaries (TP's) between zones (air void, soft and hard grout and strands) and their densities. As indicated, in this case there is more uncertainty in the boundaries C and E than in the sample 7.

Figure 6 shows the results for sample 9. The interpretation of the data is similar to that given above except that in this case the duct contains strands and the number of counts in the interval between points E and D lies below those corresponding to concrete (because of the higher density of the strands). The fact that the boundary soft-hard grout (point C) is within the zone occupied by the strands increases the uncertainty in the determination of points C and E, as indicated with a double arrow in the plot and in the tables below.

It is noteworthy that the data in Figure 6 reproduces to some extent the wavy nature expected from the lay out of the strands. This can be seen in more detail in Figure 7 where it is shown that the separation between maxima allows a determination of the diameter of the strands.

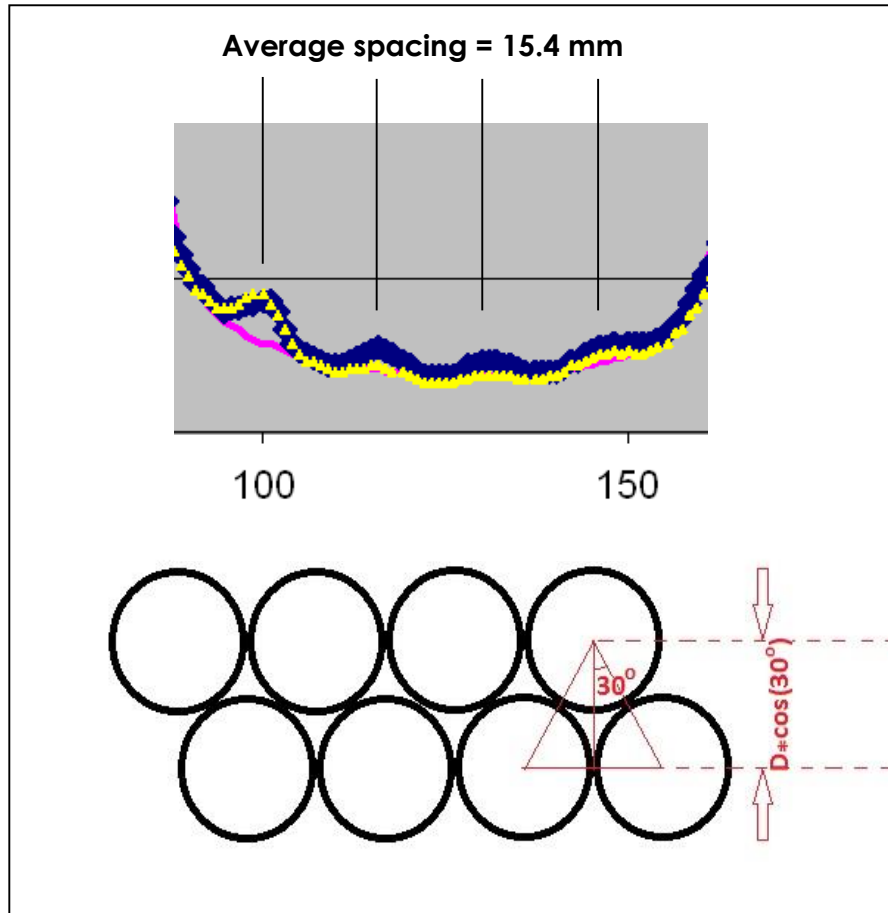


Figure 7 - Detail of strands in Sample 9. The average spacing for close-packed strands as shown in the lower part, is 15.4 mm (0.61”). This value corresponds to a diameter of each strand equal to $15.4 / \cos(30^\circ) = 17.8$ mm = 0.7 “.

CONCLUSIONS

This work shows a new technique to identify air voids and defective grouting in postensioned ducts that are embedded in large concrete structures. The method is seen to be adequate to distinguish between air voids and grout and between soft and solid grouts. In addition, the presence of strands is easily detected since the density of these elements is higher than the density of concrete and therefore the data points corresponding to a zone with strands lie well below those corresponding to concrete.

When the strands extend over the soft-hard grout interface the uncertainty in the determination of the boundaries increases from 2 mm (0.1”) to some 3.7 cm (1.5”).

ACKNOWLEDGEMENTS

The authors are grateful to Jennifer A. Grubb, Brett Holland and Paul C. Scheiner of Simpson, Gumpertz & Heger, for their help and for preparing the samples used in this work.

REFERENCES

1. Mariscotti M.A.J., Jalinoos F., Frigerio T., Ruffolo M. and Thieberger P., “Gamma-Ray Imaging for Void and Corrosion Assessment”, *ACI International*, November 2009, Vol. 31 No. 11 pp. 48-53.
2. Pimentel M., Figueiras J., Mariscotti M.A.J., Thieberger P., Ruffolo M., Frigerio T., “Gamma-ray inspection of post tensioning cables in a concrete bridge”, *Structural Faults & Repair 2010*, Edinburgh, United Kingdom, June 15 to 20, 2010.
3. THATIR was originally developed for the non-destructive determination of calcium deposits in underground pipes of the city water network. Argentine Patent AR-018132-B1, 2004.